Investigation of New 2,5-Dimethylpyrrolyl Titanium Alkylamide and Alkoxide Complexes as Precursors for the Liquid Injection MOCVD of TiO2

ARTICLE *in* CHEMICAL VAPOR DEPOSITION · MARCH 2010

Impact Factor: 1.7 · DOI: 10.1002/cvde.200906818

Chemical Vapor Deposition

DOI: 10.1002/cvde.200906818

Full Paper

Investigation of New 2,5-Dimethylpyrrolyl Titanium Alkylamide and Alkoxide Complexes as Precursors for the Liquid Injection MOCVD of TiO_2**

By *Kate Black*, *Anthony C. Jones*,* *John Bacsa*, *Paul R. Chalker*, *Paul A. Marshall*, *Hywel O. Davies*,* *Peter N. Heys*, *Paul O'Brien*, *Mohammad Afzaal*, *James Raftery*, and *Gary W. Critchlow*

The new titanium 2,5-dimethylpyrrolyl complexes $[(Me_2C_4H_2N)Ti(NMe_2)_3]$ and $[(Me_2C_4H_2N)Ti(\mu_2\text{-}O^iPr)(O^iPr)_2]_2$ and the previously reported titanium pyrrolyl complex $[(C_4H_4N)Ti(\mu_2\text{-}O^iPr)(O^iPr)_2]_2$ are synthesized and chemically and structurally characterized. Single-crystal X-ray diffraction (XRD) data show that $[(Me_2C_4H_2N)Ti(NMe_2)_3]$ is monomeric with a pseudo-tetrahedral geometry and contains an N-σ bonded 2,5-dimethylpyrrolyl ligand. The complexes $[(Me_2C_4H_2N)Ti(\mu_2\text{-}O^iPr)(O^iPr)_2]_2$ and $[(C_4H_4N)Ti(\mu_2\text{-}O^iPr)(O^iPr)_2]_2$ are dimeric and contain two terminal and two bridging isopropoxy groups and terminal N-σ-bonded pyrrolyl ligands. The complexes $[(Me_2C_4H_2N)Ti(NMe_2)_3]$ and $[(Me_2C_4H_2N)Ti(\mu_2\text{-}O^iPr)(O^iPr)_2]_2$ are investigated as precursors for the deposition of TiO_2 by liquid injection metal-organic (MO)CVD. Titanium oxide films deposited at 450 °C from $[(Me_2C_4H_2N)Ti(NMe_2)_3]$ contain significantly more carbon impurities (C = 12.7 at.-%) than those grown from $[(Me_2C_4H_2N)Ti(\mu_2\text{-}O^iPr)(O^iPr)_2]_2$ (C = 6.1 at.-%). XRD analysis shows that the titanium oxide films deposited at 450 °C are amorphous.

Keywords: MOCVD, Titanium 2,5-dimethylpyrrolyl complexes, Titanium dioxide

1. Introduction

Thin films of titanium dioxide (TiO_2) have a variety of important applications. These include high-refractive index optical coatings,[1] corrosion-protection coatings,[2] photocatalytic self-cleaning glass coatings,[3,4] biocompatible coatings,[5] dielectric capacitor layers,[6] and gate dielectric insulating films in field effect transistors (FETs).[7,8] TiO_2 is also a constituent in a number of multi-component metal oxides used in microelectronics applications, such as the high-κ dielectric oxide $(Ba,Sr)TiO_3$ for dynamic random access memory (DRAM) applications,[9] and the ferroelectric perovskites $Pb(Zr,Ti)O_3$ and $Bi_4Ti_3O_{12}$ used in infrared detectors and non-volatile ferroelectric random access memories (NV-FeRAMs).[10,11]

Various techniques have been used for the deposition of TiO_2 thin films. These include reactive sputtering,[12] ion-assisted deposition,[13] sol-gel deposition,[14] MOCVD,[15–17] and ALD.[18,19] MOCVD and ALD processes are increasingly being used as they have the advantages of good composition control, high film uniformity, good control of doping and, significantly, they give excellent conformal step coverage on highly non-planar microelectronics device geometries.

A range of precursors has been investigated for the MOCVD of TiO_2. Titanium tetrachloride ($TiCl_4$), has been widely used, in combination with O_2 or H_2O, for the MOCVD of TiO_2, [6,20–23] however $TiCl_4$ is toxic, and its use has led to chloride contamination in the TiO_2 films.[23] Titanium isopropoxide $[Ti(O^iPr)_4]$, is the most volatile titanium alkoxide,[24] and has frequently been used for the MOCVD of high-purity TiO_2 at relatively low substrate temperatures (<500 °C).[15–17,25,26] Titanium ethoxide $[Ti(OEt)_4]$, has also been investigated.[27] The anhydrous metal nitrate precursor $[Ti(NO_3)_4]$[28] and the alkylamide complex $[Ti(NMe_2)_4]$[29] have also been used for the deposition of high-purity TiO_2 by MOCVD.

The rapidly growing use of liquid injection techniques for the MOCVD of multi-component metal oxides[30] has led to the requirement for precursors with reduced air/moisture sensitivity, and for co-precursors with similar thermal

[*] Prof. A. C. Jones, Dr. K. Black, Dr. J. Bacsa
Department of Chemistry, University of Liverpool
Liverpool, L69 7ZD (UK)
E-mail: tjconsultancy@btconnect.com
Dr. H. O. Davies, Dr. P. N. Heys
SAFC Hitech, Power Road Bromborough, Wirral
Merseyside, CH62 3QF (UK)
E-mail: Hywel.Davies@sial.com
Prof. P. R. Chalker, Dr. P. A. Marshall
Department of Engineering, University of Liverpool, Liverpool,
L69 3BX (UK)
Prof. P. O'Brien, M. Afzaal, J. Raftery
School of Chemistry, University of Manchester Oxford Road,
Manchester, M13 9PL (UK)
Dr. G. W. Critchlow
Institute of Surface Science and Technology University of
Loughborough Leicestershire, LE11 3TU (UK)

[**] This work has been partly supported by the Engineering and Physical Sciences Research Council (EPSRC), UK.

stabilities. This facilitates the efficient co-evaporation of the precursors from a single evaporator, and leads to improved film uniformity.[30] Conventional Ti precursors, such as $[Ti(O^iPr)_4]$, $[Ti(NMe_2)_4]$, and $[Ti(NO_3)_4]$, are highly moisture-sensitive and have a significantly lower thermal stability than $[Ba(thd)_2]$ and $[Sr(thd)_2]$ (thd = 2,2,6,6-tetramethylheptane-3,5-dionate), which are commonly used as co-precursors for the liquid injection MOCVD of the ternary and quaternary oxides $SrTiO_3$ and $Ba(Sr,Ti)O_3$.[30] The insertion of a β-diketonate group into a metal alkoxide complex generally increases the thermal stability of the complex.[30] Consequently, the heteroleptic Ti complex $[Ti(O^iPr)_2(thd)_2]$ is now widely used in combination with $[Ba(thd)_2]$ and $[Sr(thd)_2]$ for the liquid injection MOCVD of $SrTiO_3$ and $(Ba,Sr)TiO_3$.[31,32]

The introduction of the η^5-aromatic ligand [MeCp], $[(CH_3)C_5H_4]$, has also been shown to increase the thermal stability of Ti-alkylamide complexes relative to the parent $[Ti(NR_2)_4]$ complexes. For instance, $[(MeCp)Ti(NMe_2)_3]$ allowed self-limiting ALD at substrate temperatures up to 325 °C.[33] This is significantly higher than is possible from the parent Ti-alkylamide precursor $[Ti(NMe_2)_4]$ (self-limiting ALD restricted to ~225 °C), leading, in turn, to denser, higher purity TiO_2 films. It is therefore of interest to investigate other titanium precursors for MOCVD and ALD applications which may have higher thermal stabilities than the parent $[Ti(NR_2)_4]$ or $[Ti(OR)_4]$ complexes.

Ti-alkoxide and -alkylamide complexes containing the heterocyclic pyrrolyl ligand $[C_4H_4N]$, and the methyl-substituted pyrrolyl ligand $[C_4H_{4-x}Me_xN]$, have been known for some time. These include $[(C_4H_4N)_2Ti(NR_2)_2]$ (R = Me, Et, ^{n}Pr, ^{n}Bu),[34] $[(Me_4C_4N)Ti(NMe_2)_3]$,[35] $[(Me_4C_4N)TiCl_3]$, $[(Me_4C_4N)_2TiCl_2]$, $[(Me_4C_4N)Ti(SPh)_3]$, $[(Me_4C_4N)Ti(SPh)Cl_2]$, and $[(Me_4C_4N)TiCpCl_2]$.[36] The complex $[(C_4H_4N)Ti(\mu_2\text{-}O^iPr)(O^iPr)_2]_2$ **(3)** has also been reported, but reliable characterization data were not presented.[37] A number of these Ti-pyrrolyl complexes are monomeric,[35,36] and can thus be expected to have an appreciable volatility, suitable for CVD applications. None, however, have been investigated as MOCVD precursors, and nothing is known about their thermal stability or oxide deposition temperatures. These complexes have attracted interest due to the varying bonding modes of the pyrrolyl and substituted pyrrolyl ligands, which can assume N-σ- or η^5-π-coordination modes to the Ti atom.[35,36]

In this paper we report the synthesis and characterization of the new Ti-2,5-dimethylpyrrolyl complexes $[(Me_2C_4H_2N)Ti(NMe_2)_3]$ **(1)** and $[(Me_2C_4H_2N)Ti(\mu_2\text{-}O^iPr)(O^iPr)_2]_2$ **(2)**. The Ti-pyrrolyl complex $[(C_4H_4N)Ti(\mu_2\text{-}O^iPr)(O^iPr)_2]_2$ **(3)** has also been synthesized and structurally characterized. Although **(3)** has previously been reported,[37] its molecular structure was not unambiguously established, however an N-σ-bonded pyrrolyl structure was proposed, based on ^{1}H nuclear magnet resonance (NMR) data.

Complexes **(1)** and **(2)** have been investigated as precursors for the deposition of TiO_2 thin films by liquid injection MOCVD and the results are compared to those obtained using an analogous Ti-methylcyclopentadienyl complex $[(MeCp)Ti(NMe_2)_3]$.

2. Results and Discussion

2.1. Precursor Synthesis and Characterization

Although the syntheses of several Ti-pyrrolyl complexes have been reported in the literature,[34–36] full characterization data have rarely been reported. The reaction between $[Ti(NMe_2)_4]$ and 2,5-dimethylpyrrole yields the product **(1)**, as large yellow crystals after a single distillation, however repeated attempts at purification by distillation caused decomposition, resulting in large residues of black tarry material (as yet unidentified but likely to be titanated polypyrroles). The reaction between $[Ti(NR_2)_4]$ (R = Me, Et, ^{n}Pr and ^{n}Bu) and 2,5-dimethylpyrrole was reported as early as 1968 by Bradley and Chivers,[34] however we find no evidence for the formation of Ti-bis-dimethylpyrrolyl bis-dimethylamide compounds, even when the 2,5-dimethylpyrrole/Ti ratio is increased. Complex **(1)** is stable in solution (see below and literature[34]), and can be recrystallized from the melted compound numerous times without decomposition.

A different strategy was adopted for the synthesis of the Ti^{IV} pyrrolyl alkoxides **(2)** and **(3)** using the commercially available $[TiCl(O^iPr)_3]$ starting material. We report here the facile synthesis and crystal and molecular structures of the monopyrrolyl tris-isopropoxide titanium(IV) complexes **(2)** and **(3)**. As reported in earlier studies,[37] **(3)** was found to be unstable at room temperature.

2.2. Molecular Structures

The molecular structures of **(1)**, **(2)**, and **(3)** were determined by single-crystal XRD, and are shown in Figures 1, 2 and 3, respectively, along with selected bond lengths and bond angles. Crystal and data collection parameters are given in Table 1.

Although the synthesis of the closely related tetramethyl analogue of **(1)**, namely $[(Me_4C_4N)Ti(NMe_2)_3]$, has been reported, the only molecular structure of the complex postulated to date was that of an ab-initio study.[35] The Hartree-Fock model, used in the study of $[(Me_4C_4N)Ti(NMe_2)_3]$, predicted that the most stable coordination mode of the alkylpyrrolyl ligand, was an N-σ-bonded configuration with formal π-donation of the heteroatom electron pair perpendicular to the ring plane. This σ-bonding coordination mode of the 2,5-dimethylpyrrolyl ligand is confirmed by the crystal structure of **(1)** (see Fig. 1). This is the first *tris*-alkylamide mono-pyrrolyl Ti^{IV} complex to be characterized by single-crystal XRD. The geometry around the Ti^{IV} atom is best described as distorted tetrahedral.

Chemical Vapor Deposition

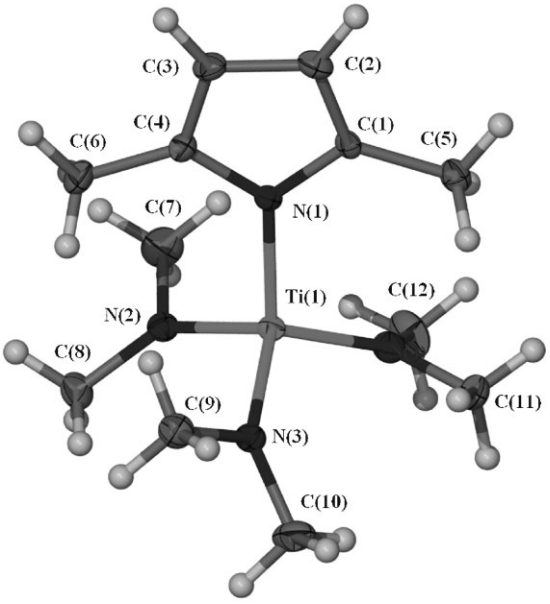

Fig. 1. The X-ray structure of **(1)**. Selected bond lengths [Å] and angles [°]: Ti(1)-N(1) 2.042(2), Ti(1)-N(2) 1.868(2), Ti(1)-N(3) 1.876(2), Ti(1)-N(4) 1.883(2); N(2)-Ti(1)-N(3) 105.39(9), N(2)-Ti(1)-N(4) 108.88(8), N(3)-Ti(1)-N(4) 109.55(8), N(2)-Ti(1)-N(1) 107.02(8), N(3)-Ti(1)-N(1) 111.81(8), N(4)-Ti(1)-N(1) 113.78(8).

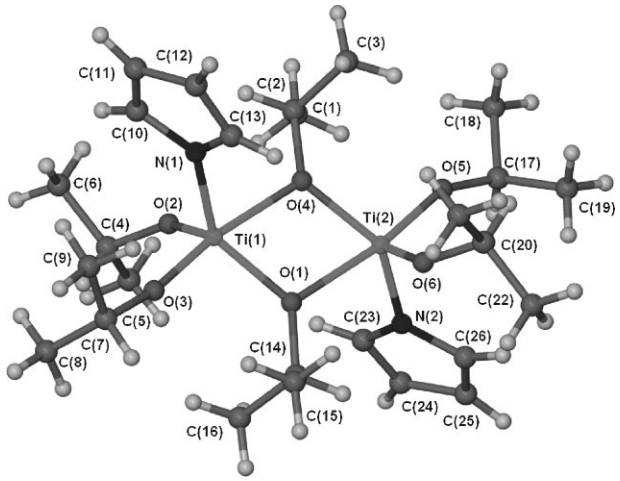

Fig. 3. The X-ray structure of **(3)**. Selected bond lengths [Å] and bond angles [°]: Ti(1)-O(1) 1.9456(13), Ti(1)-O(4) 2.0885(12), Ti(2)-O(4) 1.9369(13), Ti(2)-O(1) 2.0982(12), Ti(1)-N(1) 2.0199(17), Ti(1)-O(2) 1.7695(13), Ti(1)-O(3) 1.7644(14), Ti(2)-O(1) 2.0982(12), Ti(2)-O(5) 1.7730(13), Ti(2)-O(6) 1.7769(13), Ti(2)-N(2) 2.0169(16), O(1)-C(14) 1.455(3), O(2)-C(4) 1.433(2); O(1)-Ti(1)-O(2) 114.63(6), O(1)-Ti(1)-O(3) 98.03(6), O(1)-Ti(1)-O(4) 72.50(5), O(1)-Ti(1)-N(1) 132.16(6), O(2)-Ti(1)-O(3) 101.49(6), O(2)-Ti(1)-O(4) 93.51(6), O(2)-Ti(1)-N(1) 108.01(7), O(3)-Ti(1)-O(4) 164.67(6), O(3)Ti(1)-N(1) 93.72, O(4)-Ti(1)-N(1) 84.53(6).

There is a slight deviation from ideal T_d symmetry, with the N(pyrrolyl)-Ti-N(alkylamide) angles showing the greatest deviation from 109.5° [N(3)-Ti(1)-N(1) = 111.81(8)° and N(4)-Ti(1)-N(1) = 113.78°]. It is also worth noting that the Ti-N(pyrrolyl) bond distance (2.042(2) Å) is longer than the three Ti-N(alkylamide) bonds (1.868(2), 1.876(2), 1.883(2) Å) indicating that the pyrrolyl ligand forms weaker coordination bonds to Ti cations than the dimethylamide anions. Although the angles between the Ti atom and the dimethylamide ligands all have values close to ideal tetrahedral geometry, the angles involving the 2,5-dimethylpyrrolyl ligand are larger. This is likely to be due to steric repulsion between the methyl substituents of the pyrrolyl ring and the alkylamide methyl groups. The η^5 coordination of such alkylpyrrolyl rings has previously been addressed for complexes of general formula $[Ti(\eta^5\text{-}NC_4Me_4)L_3]$ for L = Cl, SPh.[37]

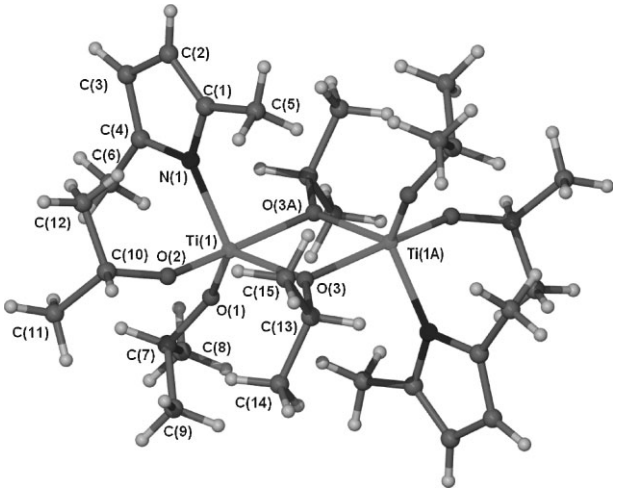

Fig. 2. The X-ray structure of **(2)**. Selected bond lengths [Å] and angles [°]: Ti(1)-O(3) 1.938(2), Ti(1)-O(3A) 2.108(2), Ti(1A)-O(3) 2.108(2), Ti(1A)-O(3A) 1.938(2), Ti(1)-N(1) 2.012(3), Ti(1)-O(1) 1.768(2), Ti(1)-O(2) 1.763(2), O(1)-C(7) 1.427(4), O(3)-C(13) 1.452(6), C(13)-C(15) 1.487(8), O(2)-C(10) 1.405(8), O(2)-Ti(1)-O(1) 101.5(1), O(2)-Ti(1)-O(3) 98.2(1), O(1)-Ti(1)-O(3) 115.0(1), O(2)-Ti(1)-N(1) 93.4(1), O(1)-Ti(1)-N(1) 109.3(1), O(3)-Ti(1)-N(1) 130.5(1), O(2)-Ti(1)-O(3A) 166.83(1), O(1)-Ti(1)-O(3A) 90.7(1), O(3)-Ti(1)-O(3A) 72.0(1), N(1)-Ti(1)-O(3A) 86.9(1).

Complexes **(2)** and **(3)** are the first structurally characterized titanium pyrrolyl alkoxide complexes. XRD data show that both **(2)** and **(3)** are dimeric molecules containing μ-isopropoxy groups bridging the Ti^{IV} centers. Complex **(2)** is centrosymmetric with the Ti^{IV} atoms lying on an inversion centre, and the inversion-related Ti(1), Ti(1A), O(3), and O(3A) atoms are labeled in Figure 2. Complex **(3)** is not centrosymmetric, as the molecule does not lie on an inversion centre despite the $Ti_2O_6N_2$ core clearly having inversion symmetry (C_i). Some of the positive charge of the Ti^{IV} atoms is transferred to the bridging ligands and to their hydrogen atoms. The loss in symmetry may be due to the complex network of weak interactions between the pyrollyl and alkoxy H atoms. In **(2)** and **(3)** each Ti^{IV} atom is five-coordinated, being coordinated to two terminal and two bridging μ-isopropoxy groups, and one terminal pyrrolyl group. In both **(2)** and **(3)**, the μ-isopropoxy O atom bridges the metal atoms asymmetrically, with the O atom forming one long and one short bond to the Ti^{IV} atom (1.938(2) and

Table 1. Crystallographic Data for Complexes (**1**), (**2**), and (**3**).

	(**1**)	(**2**)	(**3**)
Mol. formula	$C_{12}H_{26}N_4Ti$	$C_{30}H_{58}N_2O_6Ti_2$	$C_{26}H_{50}N_2O_6Ti_2$
Formula weight	274.27	638.58	582.48
Colour, shape	Yellow, prism	Red, prism	Yellow, prism
Dimensions [mm]	$0.5 \times 0.4 \times 0.2$	$0.32 \times 0.22 \times 0.15$	$0.5 \times 0.4 \times 0.3$
Diffractometer	Bruker Smart Apex	Bruker Smart Apex	Bruker D8
Temp [K]	100(2)	100(2)	100(2)
Crystal system	Monoclinic	Triclinic	Monoclinic
Space group	$P2_1/c$	P-1	$P2_1/c$ (No. 14)
a [Å]	9.6612(16)	9.2968(11)	17.502(2)
b [Å]	14.7836(18)	9.8511(12)	12.306(1)
c [Å]	11.259(7)	11.4999(14)	16.608(2)
α [°]	90.00	91.864(2)	90.00
β [°]	110.64(4)	112.704(2)	117.945(2)
γ [°]	90.00	113.038(2)	90.00
V [Å^3]	1504.9(10)	872.95(18)	3160.2(6)
Z	4	1	4
F(000)	592	344	1248
D_{calc} [g cm^{-3}]	1.211	1.215	1.224
Radiation, λ(Mo-Kα) [Å]	0.71073	0.71073	0.71073
T_{min}/T_{max}	0.8969/0.6646	0.9292/0.8572	0.8542/0.7732
θ range [°]	3.71 to 26.37	1.97 to 28.27	1.32 to 27.10
Completeness of data set [%]	99.7	99.4	98.5
No. of measured reflections	9044	7589	17822
No. of unique reflections	3062	3958	6878
R(int)	0.0408	0.0678	0.0211
No. of parameters	162	189	337
Final R(F_{hkl}): R_1	0.0366	0.0664	0.0376
ωR_2	0.0751	0.1104	0.0957
Goodness of fit	1.066	0.896	1.047
ρ_{max}/ρ_{min} [e Å^{-3}]	0.346/-0.412	0.613/-0.367	1.082/-0.488

2.108(2) Å in **(2)**) and (1.9456(13), 1.9369(13) and 2.0885(12), 2.0982(12) Å in **(3)**). This asymmetric coordination is a result of an electronic effect; a second-order, Jahn-Teller distortion[38] that arises from a mixing of the filled p orbitals on the oxygen ligands with the empty d orbitals of the metal. The bridging Ti-^{i}OPr bonds in **(2)** and **(3)** are significantly longer than the terminal Ti-O^{i}Pr bonds (1.763(2) – 1.7769(13) Å), but the bond valence sum of the Ti-O-Ti bond pair across the Ti-Ti inter-nuclear axis is equal to the valence of a single terminal Ti-O bond (1.1 v.u.). There is also a lengthening of the bridging Ti-O^{i}Pr oxyalkane O-C bond compared with the terminal O^{i}Pr ligands. The long C-O bonds (e.g., O(3)-C(13) 1.452(6) Å in **(2)**, and O(1)-C(14) 1.455(3) Å in **(3)**) indicate that positive charge is being transferred to the oxyalkane moiety. The coordination environment of each titanium atom in both structures is best described as trigonal bipyramidal with a large distortion towards square pyramidal geometry along a Berry pseudo-rotation coordinate (pivot atom O(1) in **(2)**, and O(5) and O(3) in **(3)**). The coordination environment of the titanium is completed by an N-σ-bonded pyrrolyl ligand, which is consistent with the other structures reported here. The Ti-N bonds in **(2)** and **(3)** are comparable in length (2.012(3), 2.0199(17) Å, respectively) to the Ti-$NC_5H_4Me_2$ bond in **(1)** (2.042(2) Å), indicating that the Ti-N bonds in each complex have similar strengths.

2.3. Thermogravimetric Analysis (TGA)

The evaporation characteristics of complexes were assessed by TGA and the data are shown in Figure 4. TGA data provide an indication of the volatility and decomposition characteristics of a complex.[39]

Complexes **(2)** and **(3)** show a significant loss of mass over the temperature range $\sim$100 – 260 °C and $\sim$100 – 240 °C, respectively. In each case, a significant amount of residue (5.7 – 6.0%) remained, probably due to the formation of TiO_2. The remaining residues, however, are significantly less

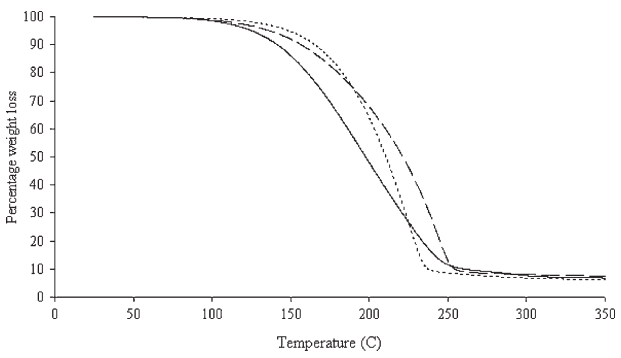

Fig. 4. TGA data for **(1)** (– – –), **(2)** (—), and **(3)** (. . .).

than would result if full decomposition to the oxide had occurred (e.g., **(2)** 25% TiO_2, **(3)** 27.5% TiO_2). This indicates that the observed mass loss in the TGA is due principally to evaporation of the complexes.

Complex **(1)** shows significant mass loss over the temperature range ~100 – 260 °C, with a residue of 7.1%, possibly due to the formation of TiN and/or TiC_xN_y. This residue is significantly less than expected if full decomposition to the nitride or carbonitride had occurred (~22%), which indicates that the observed mass loss in the TGA data is mainly due to evaporation of the complex.

It is noteworthy that the dimeric complex **(2)** evaporates at similar temperatures to the monomeric complex **(1)** (~100 – 260 °C). This suggests that the longer and weaker bridging Ti-O^{i}Pr bonds in **(2)** (Ti(1)-O(3A) and Ti(1A)-O(3) in Fig. 2) cleave to form a monomeric species, $[(Me_2C_4H_2N)Ti(\mu_2\text{-}O^iPr)(O^iPr)_2]$, during the evaporation process. The dimeric complex **(3)** evaporates at slightly lower temperatures (~100 – 240 °C) than **(1)** and **(2)**, which also suggests that complex **(3)** becomes monomeric during evaporation due to cleavage of the weaker bridging Ti-O^{i}Pr bonds (Ti(1)-O(4) and Ti(2)-O(1) in Fig. 3).

2.4. MOCVD of TiO_2 Thin Films

Despite promising TGA data, complex **(3)** was found to decompose at room temperature under an inert atmosphere over time to give a black tar. Consequently, it was considered unsuitable for MOCVD applications, however complexes **(1)** and **(2)** were found to be stable at room temperature and suitable for the liquid injection MOCVD of TiO_x films over a wide range of substrate temperatures.

The variation in growth rate with substrate temperature of the TiO_x films grown from complexes **(1)** and **(2)** and $[(MeCp)Ti(NMe_2)_3]$ is shown in Figure 5. For each complex, three regions of growth are evident. For complex **(1)**, the onset of oxide growth occurs at ~250 °C and then increases rapidly up to ~350 °C. This corresponds to the region of kinetic control in which the film growth rate is controlled by the thermal decomposition of the precursor on the substrate or in the boundary layer adjacent to the substrate. The oxide growth rate then reaches a maximum in the temperature range 350 – 460 °C, corresponding to a fairly broad region of diffusion-controlled growth from a fully decomposed precursor. At substrate temperatures above ~460 °C, the oxide growth rate decreases rapidly due to precursor depletion in the gas phase or on the reactor walls.

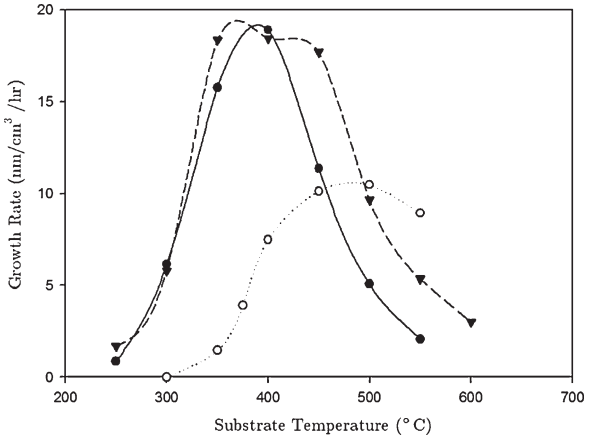

Fig. 5. Variation of growth rate with substrate temperature for TiO_x films grown by MOCVD using **(1)** (▼), **(2)** (○), and $[(MeCp)Ti(NMe_2)_3]$ (●).

Temperatures for the onset of oxide growth and kinetically controlled growth from $[(MeCp)Ti(NMe_2)_3]$ are similar to those observed for complex **(1)**, suggesting that the complexes have comparable thermal stabilities, however, the oxide growth rate from $[(MeCp)Ti(NMe_2)_3]$ decreases much more rapidly above 400 °C, giving a much narrower region of diffusion-controlled growth compared to **(1)**, indicating more rapid depletion of the complex in the gas-phase and/or on the reactor walls at high temperature.

For complex **(2)**, the onset of oxide growth occurs at a higher temperature (~300 °C) than either **(1)** or $[(MeCp)Ti(NMe_2)_3]$. The region of kinetically controlled growth also occurs at higher temperatures (~300 – 450 °C), indicating that this complex has the highest thermal stability of the three examined. Complex **(3)** also gives a fairly broad region of diffusion-controlled growth, from ~450 – 550 °C, above which temperature the oxide growth rate decreases. These observations imply that the replacement of the $[NMe_2]$ groups on **(1)** by the alkoxide groups $[O^iPr]$ increases the thermal stability of the complex. A further factor leading to the increased thermal stability of **(2)** may be its dimeric nature, although at evaporation temperatures of 130 °C and substrate temperatures > 300 °C, the molecule is unlikely to remain dimeric. ALD studies[33] have established that $[(MeCp)Ti(NMe_2)_3]$ has one of the highest thermal stabilities of the available Ti CVD precursors, and the growth data presented in Figure 5 indicates that the 2,5-dimethylpyrrolyl complexes **(1)** and **(2)** also have relatively high thermal stabilities.

These apparent trends in precursor thermal stability for the organometallic Ti complexes are broadly consistent with thermal stability trends previously observed for Zr and Hf alkylamides, and alkoxides used in liquid injection MOCVD studies. For instance, the alkoxides $[M(O^tBu)_2(mmp)_2]$, $[M(mmp)_4]$ (M = Zr,Hf; mmp = $OCMe_2OMe$),[40] show oxide growth onset temperatures of ~350 °C and a region of kinetic control of ~350 – 550 °C, whereas $[Hf(NMe_2)_4]$ exhibits an onset temperature of ~200 °C with the region of kinetic control of ~200 – 300 °C,[41] indicative of a considerably lower thermal stability.

The atomic composition of the TiO_x films grown at 450 °C from **(1)** and **(2)** was determined by Auger electron spectroscopy (AES) and the data are shown in Table 2, together with AES data for $[(MeCp)Ti(NMe_2)_3]$. The films deposited from all three precursors are highly sub-stoichio-

Table 2. Composition of TiO_x films [at.-%] deposited by MOCVD ($T_g = 450\,^{\circ}C$) using **(1)**, **(2)**, and $[(MeCp)Ti(NMe_2)_3]$.

Film No.	Ti precursor	Ti	O	C	O/Ti ratio
S1446	**(1)**	40.5	46.8	12.7	1.15
S1448	**(2)**	41.0	52.9	6.1	1.29
S1415	$[(MeCp)Ti(NMe_2)_3]$	40.2	47.1	12.7	1.17

Table 3. Growth conditions used for the deposition of TiO_x films by liquid injection MOCVD using **(1)**, **(2)**, and $[(MeCp)Ti(NMe_2)_3]$.

Solvent	Toluene
Precursor concentration	0.05 M
Evaporator temperature	100 °C
Pressure	5 mbar
Argon flow rate	200 $cm^3\,min^{-1}$
Substrates	Si(100)
Substrate temperature(s)	250 °C to 600 °C
Oxygen flow rate	100 $cm^3\,min^{-1}$

metric, with O/Ti ratios of 1.15 – 1.29. These O/Ti ratios are significantly lower than those previously reported for TiO_2 films deposited by MOCVD using Ti-alkoxide precursors such as $[Ti(O^iPr)_3(dmae)]$ (1.62 – 1.82),[42] $[Ti(O^iPr)_2(dmae)_2]$ (1.62 – 1.74),[42] $[Ti(OCMe_2CMe_2O)(dmae)_2]_2$ (1.33 – 1.60) ($dmae = OCH_2CH_2NMe_2$).[43] Non-stoichiometric oxide films are frequently produced by MOCVD processes involving metal alkoxide precursors,[42,44] and stoichiometric oxide films can readily be obtained by a post-growth anneal in air or oxygen at 600 – 1000 °C.[45]

The TiO_x films deposited from **(1)** and $[(MeCp)Ti(NMe_2)_3]$ show a high level of carbon contamination (C = 12.7 at.-%). Significantly, carbon was reportedly absent in TiO_2 films grown by MOCVD using $[Ti(NMe_2)_4]$,[29] suggesting that the major route to carbon incorporation is the decomposition of the [2,5-dimethylpyrrolyl] and the [MeCp] ligands. In contrast, significantly lower carbon levels were detected in the TiO_x films grown using **(2)** (C = 6.1 at.-%). We propose that, during the pyrolysis of $[(Me_2C_4H_2N)Ti(\mu_2\text{-}O^iPr)(O^iPr)_2]_2$, a β-hydrogen is transferred from $[O^iPr]$ to the $[Me_2C_4H_2N]$ group leading to the more facile elimination of $[Me_2C_4H_2NH]$, as well as the elimination of $[CH_2=CHCH_3]$ and the formation of [Ti-O] bonds (see Fig. 6).The facile β-hydride elimination of the two other $[O^iPr]$ groups leads, in turn, to the deposition of TiO_x. Support for this proposal is provided by previous MOCVD studies using $[MeZn(O^iPr)]$[46] which indicated that transfer of a β-hydrogen from $[O^iPr]$ to a [Zn-Me] group leads to the liberation of $[CH_2=CHCH_3]$ and the facile elimination of the hydrocarbon group $[CH_4]$. The carbon levels in the TiO_x films grown from **(2)** are comparable to those observed in TiO_x films grown by MOCVD using Ti alkoxides such as $[Ti(O^iPr)_3(dmae)]$ (C = 2.9 – 7.7 at.-%),[31] $[Ti(O^iPr)_2(dmae)]$ (C = 3.1 – 6.7 at.-%),[31] $[Ti(OCMe_2CMe_2O)(dmae)_2]_2$ (C = N.D. – 6.0 at.-%).[32] AES is not sensitive to traces of nitrogen in the films, and so we are unable to confirm its presence, or otherwise, in the present studies.

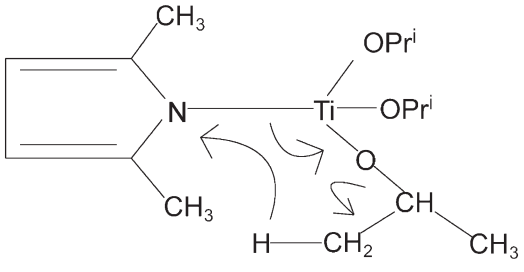

Fig. 6. Mechanism proposed for the elimination of the [2,5-dimethylpyrrolyl] ligand from complex **(2)**.

XRD spectra of the TiO_x films deposited at 450 °C from **(1)**, **(2)** and $[(MeCp)Ti(NMe_2)_3]$ were featureless, indicating that the films were essentially amorphous.

3. Conclusions

Thin films of TiO_x have been deposited by liquid injection MOCVD using the new Ti-2,5-dimethylpyrrolyl complexes **(1)** and **(2)**. The MOCVD growth data suggest that these complexes have higher thermal stabilities than $[(MeCp)Ti(NMe_2)_3]$, however high levels of carbon (C = 12.7 at.-%) were observed in TiO_x films grown using **(1)**, which we attribute to the decomposition of the [2,5-dimethylpyrrolyl] ligand. Lower carbon levels were observed in films deposited using **(2)** (C = 6.1 at.-%), and it is proposed that the presence of the $[O^iPr]$ group in **(2)** leads to a cleaner, more facile elimination of [2,5-dimethylpyrrolyl] via an intramolecular β-hydrogen abstraction resulting in the deposition of higher purity TiO_x films.

4. Experimental

General Techniques: All manipulations were carried out under an atmosphere of dry nitrogen using standard Schlenk line or dry-box techniques. Dry solvents and other starting materials were supplied by Sigma Aldrich Ltd and were purified where necessary. ^1H NMR spectroscopy was carried out on a Bruker Avance 400 NMR spectrometer (^1H 400.1 MHz). TGA was carried out on a Mettler Toledo thermogravimetric analyzer in a nitrogen-filled glove box. Nitrogen flow was maintained at 50 L min^{-1} and samples were held in platinum crucibles.

AES was carried out on a Varian scanning Auger spectrometer. The atomic compositions quoted are from the bulk of the film (typically 70 – 80 nm depth), free from surface contamination, and were obtained by combining AES with sequential argon ion bombardment until comparable compositions were obtained for consecutive data points. Compositions were based on a TiO_2 powder reference.

Precursor Synthesis: **(1).** A solution of 2,5-dimethylpyrrole (2.39 g, 25 mmol) in toluene (10 mL) was added to a solution of $[Ti(NMe_2)_4]$ (5.63 g, 25 mmol) in toluene (20 mL) over a period of 30 min. The solution was kept at 90 °C for 3 h and then stirred overnight at room temperature. The toluene was removed in-vacuo and the dark brown liquid distilled. Distillation proved somewhat difficult with conditions starting at 70 °C/0.1 mm Hg and rising to 110 °C/0.1 mm Hg as the distillation progressed. The

product is isolated as a dark yellow, low melting solid (mpt ~20 °C). ^{1}H NMR (d_6-benzene, δ ppm): 2.35 (CH_3 of $Me_2C_4H_2N$, singlet, 6H), 3.1 ($N(CH_3)_2$, singlet, 18H), 6.1 (H of $Me_2C_4H_2N$, singlet, 2H).

(2): $[TiCl(O^iPr)_3]$ (15.77 mL, 1 M hexane solution) was added dropwise from a syringe to a hexane suspension of lithium 2,5-dimethylpyrrole (prepared at −30 °C and used in-situ by reacting 10 mL 1.6 M ^{n}BuLi with 1.5 g 2,5-dimethylpyrrole). The mixture immediately turned dark orange and was stirred for 3 h at room temperature. The mixture was allowed to settle overnight before removing the mother liquor by filtration. The LiCl by-product was washed with 2 × 10 mL *n*-hexane and then the hexane was removed in-vacuo until incipient crystallization occurred. The product was obtained as large red crystals. ^{1}H NMR (d_6-benzene, δ ppm): 1.1 (CH_3 of O^iPr, doublet, 18H), 2.3 (CH_3 of $Me_2C_4H_2N$, s, 6H), 4.2 (CH of O^iPr, septet, 3H), 6.0 (H of $Me_2C_4H_2N$, singlet, 2H).

(3): $[TiCl(O^iPr)_3]$ (15.65 mL, 1 M hexane solution) was added dropwise from a syringe to a hexane suspension of lithium pyrrole (prepared at −30 °C and used in-situ by reacting 10 mL 1.6 M ^{n}BuLi with 1.05 g pyrrole). The mixture immediately turned dark orange and was stirred for 3 h at room temperature. The mixture was allowed to settle for 24 h before removing the mother liquor by filtration. The LiCl by-product was washed with 2 × 10 mL *n*-hexane and then hexane was removed in-vacuo until incipient crystallization occurred. Storage at −20 °C yielded the product as large yellow crystals. ^{1}H NMR (d_6-benzene, ppm): 1.1 (CH_3 of O^iPr, doublet, 18H), 4.4 (CH of O^iPr, septet, 3H), 6.45 (H of C_4H_4N, singlet, 2H) and 7.25 (H of pyrrolyl, singlet, 2H)

Single-crystal XRD: Crystallographic data for **(1)** and **(2)** were obtained using a Bruker Smart APEX CCD diffractometer using graphite monochromated Mo Kα radiation ($\lambda = 0.71073$ Å, $T = 150$ K). The structure was solved by direct methods and refined by full-matrix least squares against F^2 using all data [47]. Non-hydrogen atoms were refined anisotropically, and H-atoms were fixed in geometrically ideal positions. Crystallographic data for **(3)** were obtained using a Bruker D8 diffractometer with an APEX CCD detector using graphite monochromated Mo Kα radiation ($\lambda = 0.71073$ Å, $T = 100$ K). The structure was solved by direct methods and refined by full-matrix least squares against F^2 using all data [47]. Non-hydrogen atoms were refined anisotropically, and H-atoms were fixed in geometrically ideal positions. Crystallographic data (excluding structure factors) for the structures reported in this paper have been deposited with the Cambridge Crystallographic Data Centre (CCDC) as supplementary publication numbers CCDC 704352 **(1)**, 704351 **(2)**, and 710796 **(3)**.

MOCVD and ALD Studies: Liquid injection MOCVD experiments were carried out on an Aixtron AIX 200FE AVD reactor fitted with a modified liquid injection system [48]. The substrate was rotated throughout the MOCVD experiments. Thin films of TiO_x were deposited on Si(100) substrates using 0.05 M toluene solutions of complexes **(1)**, **(2)** and $[(MeCp)Ti(NMe_2)_3]$ in the presence of oxygen. The growth conditions are shown in Table 3. Film thicknesses were calculated by mass gain assuming a density of 3.895 g cm^{-3} for TiO_2.

Received: June 3, 2009
Revised: August 14, 2009

[1] J. M. Bennett, E. Pelletier, G. Albrand, J. P. Borgogno, B. Lazarides, C. K. Carniglia, R. A. Schmell, T. H. Allen, T. Tuttle-Hart, K. H. Guenther, A. Saxer, *Appl.Opt.* **1989**, *28*, 3303.

[2] R. Matero, M. Ritala, M. Leskelä, T. Salo, J. Aromaa, O. Forsén, *J. Phys. IV* **1999**, *9*, Pr8-493.

[3] A. Mills, A. Lepre, N. Elliott, S. Bhopal, I. P. Parkin, S. A. O'Neill, *J. Photochem. Photobiol, A* **2002**, *148*, 213.

[4] I. P. Parkin, R. G. Palgrave, in: *Chemical Vapour Deposition, Precursors, Processes and Applications* (Eds: A. C. Jones, M. L. Hitchman) Royal Society of Chemistry, Cambridge 2008, Ch. 10, Section 10.6.

[5] J. Wu, S. Hayakawa, K. Tsuru, A. Osaka, *Thin Solid Films*, **2002**, *414*, 283.

[6] A. E. Feuersanger, *Proc. IEEE* **1964**, *52*, 1463.

[7] H. S. Kim, D. C. Gilmer, S. A. Campbell, D. L. Polla, *Appl. Phys. Lett.* **1996**, *69*, 3860.

[8] J. Yan, D. C. Gilmer, S. A. Campbell, W. L. Gladfelter, P. G. Schmid, *J. Vac. Sci. Technol,B* **1996**, *14*, 1706.

[9] E. Ezhilvalavan, T.-Y. Tseng, *Mater. Chem. Phys* **2000**, *65*, 227.

[10] O. Aucellio, C. M. Foster, R. Ramesh, *Ann. Rev. Mater. Sci.* **1998**, *28*, 501.

[11] T. Kijima, H. Matsunaga, *Jpn. J. Appl. Phys.* **1998**, *37*, 5171.

[12] T. K. Lakshman, C. A. Wisocki, W. J. Slegesky, *IEEE Comp.* **1964**, Parts Cp-11 (2), 14.

[13] F. L. Williams, J. J. McNally, G. A. Al-Jumaily, J. R. McNeil, *J. Vac. Sci. Technol, A* **1987**, *5*, 2159.

[14] H. J. Hovel, *J. Electrochem. Soc.* **1978**, *125*, 983.

[15] E. T. Fitzgibbons, K. J. Sladek, W. H. Hartwig, *J. Electrochem. Soc.* **1972**, *119*, 735.

[16] C. P. Fictorie, J. F. Evans, W. L. Gladfelter, *J. Va. Sci. Technol A* **1994**, *12*, 1108.

[17] N. Rausch, E. P. Burte, *J. Electrochem. Soc.* **1993**, *140*, 145.

[18] M. Ritala, M. Leskelä, E. Nykänen, P. Soininen, L. Niinistö, *Thin Solid Films* **1993**, *225*, 288.

[19] V. Pore, A. Rahtu, M. Lekskelä, M. Ritala, T. Sajavaara, J. Keinonen, *Chem. Vap. Deposition* **2004**, *10*, 143.

[20] G. Haas, *Vacuu*, **1952**, *2*, 331.

[21] R. N. Goshtagore, *J. Electrochem. Soc.* **1970**, *117*, 529.

[22] S. Hayashi, T. Hirai, *J. Crystal Growth* **1976**, *36*, 157.

[23] L. M. Williams, D. W. Hess, *J. Vac. Sci. Technol, A* **1983**, *1*, 1810.

[24] D. C. Bradley, R. C. Mehrotra, D. P. Gaur, *Metal Alkoxides*, Academic Press, New York 1978.

[25] M. Yokozawa, H. Iwasa, I. Teramoto, *Jpn. J. Appl. Phys.* **1968**, *7*, 96.

[26] J. P. Lu, J. D. Wang, R. Raj, *Thin Solid Films* **1991**, *204*, L13.

[27] S. Sakurai, M. Watanabe, *Rev. Elect. Commun. Lab.* **1963**, *11*, 178.

[28] R. C. Smith, T. Z. Ma, N. Hoilien, L. Y. Tsung, M. J. Bevan, L. Colombo, J. Roberts, S. A. Campbell, W. L. Gladfelter, *Adv. Mater. Opt. Electron.* **2000**, *10*, 105.

[29] J. B. Woods, D. B. Beach, C. L. Nygren, Z. L. Xue, *Chem. Vap. Deposition* **2005**, *11*, 289.

[30] A. C. Jones, *J. Mater. Chem.* **2002**, *12*, 2576.

[31] J. F. Roeder, T. H. Baum, S. M. Bilodeau, G. T. Stauf, C. Ragaglia, M. W. Russell, P. C. Van Buskirk, *Adv. Mater. Opt. Electron.* **2000**, *10*, 145.

[32] J.-P. Sénateur, C. Dubourdieu, F. Weiss, M. Rosina, A. Arbrutis, *Adv. Mater. Opt. Electron.* **2000**, *10*, 155.

[33] P. A. Williams, A. Kingsley, T. Leese, P. N. Heys, Y. Otsuka, K. Uotani, *Paper Presented at AVS-ALD 2008 Conf. Bruges, Belgium,* June 29th – July 2nd, **2008**.

[34] D. C. Bradley, K. J. Chivers, *J. Chem. Soc, A* **1968,** 1967.

[35] A. R. Dias, A. M. Galvão, A. C. Galvão, *Collect. Czech. Chem. Commun.* **1998**, *63*, 182.

[36] A. R. Dias, A. M. Galvão, A. C. Galvão, M. S. Salema, *J. Chem. Soc, Dalton Trans.* **1997**, 1055.

[37] R. Choukroun, D. Gervais, *Synth. React. Inorg. Met. -Org. Chem.* **1978**, *8*, 137.

[38] A. Kucht, H. Kucht, S. Barry, J. C. W. Chien, M. D. Rausch, *Organometallics* **1993**, *12*, 875.

[39] S. E. Potts, C. J. Carmalt, C. S. Blackman, T. Leese, H. O. Davies, *J. Chem. Soc, Dalton Trans.* **2008**, 5730.

[40] P. A. Williams, J. L. Roberts, A. C. Jones, P. R. Chalker, N. L. Tobin, J. F. Bickley, H. O. Davies, L. M. Smith, T. J. Leedham, *Chem. Vap. Deposition* **2002**, *8*, 163.

[41] P. A. Williams, A. C. Jones, N. L. Tobin, P. R. Chalker, S. Taylor, P. A. Marshall, J. F. Bickley, L. M. Smith, H. O. Davies, G. W. Critchlow, *Chem. Vap. Deposition* **2003**, *9*, 309.

[42] A. C. Jones, T. J. Leedham, P. J. Wright, M. J. Crosbie, K. A. Fleeting, D. J. Otway, P. O'Brien, M. E. Pemble, *J. Mater. Chem.* **1998**, *8*, 1773.

[43] A. C. Jones, P. A. Williams, J. F. Bickley, A. Steiner, H. O. Davies, T. J. Leedham, A. Awaluddin, M. E. Pemble, G. W. Critchlow, *J. Mater. Chem.* **2001**, *11*, 1428.

[44] M. J. Crosbie, P. J. Wright, D. J. Williams, P. A. Lane, J. Jones, A. C. Jones, T. J. Leedham, P. O'Brien, H. O. Davies, *J. Phys. IV* **1999**, *9*, Pr8-935.

[45] K. D. Pollard, R. J. Puddephat, *Chem. Mater.* **1999**, *11*, 1069.

[46] J. Auld, D. J. Houlton, A. C. Jones, S. A. Rushworth, M. A. Malik, P. O'Brien, G. W. Critchlow, *J. Mater. Chem.* **1994**, *4*, 1249.

[47] G. M. Sheldrick, *SHELXS-97, Program for Solution of Crystal Structures*, University of Göttingen, Germany 1997.

[48] R. J. Potter, P. R. Chalker, T. D. Manning, H. C. Aspinall, Y. F. Loo, A. C. Jones, L. M. Smith, G. W. Critchlow, M. Scumacher, *Chem. Vap. Deposition* **2005**, *11*, 159.

